THE DYNAMICS OF LIQUID MOVEMENT INSIDE THE NOZZLE DURING THE BUBBLE DEPARTURES FOR LOW AIR VOLUME FLOW RATE

Paweł DZIENIS*, Romuald MOSDORF*, Tomasz WYSZKOWSKI*

*Białystok University of Technology, Faculty of Mechanical Engineering, Department of Mechanics and Applied Computer Science.
ul. Wiejska 45C, 15-351 Białystok, Poland

dzienis.pawel@gmail.com, mosdorf@gmail.com, wyszkowski.tomasz@gmail.com

Abstract: The main aim of investigation was to analyze the influence of liquid movement inside the nozzle on the dynamics of bubble departure. Dynamics of such process decides about the periodic and aperiodic bubble departures. During the experiment it has been simultaneously recorded: changes of the depth of the nozzle penetration by liquid, air pressure and shape of bubble trajectory directly over the nozzle (in the length of 30 mm). The air volume flow rate was in the range 0.00632 - 0.0381 l/min. There has been shown that for all air volume flow rates the time periods with periodic and aperiodic bubble departures have been occurred. Duration of these intervals varies with the air volume flow rate. It has been found that the aperiodic bubble departures begin when the time of bubble growth increases. The changes of maximum values of liquid position inside the nozzle are associated with changes of the shape of bubble trajectories. There has been shown that straightens of the trajectory precedes the appearance of periodical or aperiodic time period of bubble departures. The aperiodic bubble departures are accompanied by a significant deviation of bubble trajectory from a straight line. The correlation dimension analysis shown that three independent variables are enough to describe the behaviour of liquid movement inside the nozzle. These independent variables may be: liquid velocity, liquid position in the nozzle and gas pressure in the nozzle.

Keywords: Bubbles, Nonlinear Analysis

1. INTRODUCTION

The time period between two subsequent bubbles departing from the nozzle may be divided into two periods: waiting time and time of the bubble growth. During the waiting time for the low frequency of bubble departures the nozzle is flooded by liquid. Then, the liquid is removed from the nozzle, because the gas pressure inside a gas supply system increases (Koval'chuk et al., 1999). Dynamics of such process decides about the periodic and aperiodic bubble departures.

There are a lot of papers reporting the non-linear behaviours of the bubbling process. It has been found that the meniscus oscillations in orifice strongly affect the subsequent bubble cycles (Ruzicka et al., 2009a, b). The analyses carried out in (Ruzicka et al., 2009a) show that ways of chaos appearance in bubbling depend on the nozzle or orifice diameter (Stanovsky et al., 2011; Cieslinski and Mosdorf, 2005; Mosdorf and Shoji, 2003; Koval'chuk et al., 1999; Zang and Shoji, 2001). The influence of: plate thickness, surface tension, viscosity of the liquid and the height of liquid column on the length of liquid penetration inside the nozzle have been reported in the papers (Ruzicka et al., 2009a, b; Dukhin et al., 1998a, b; Koval'chuk et al., 1999). In Stanovsky et al. (2011) the influence of orifice diameter on the depth of liquid penetration inside the orifice has been investigated. In Stanovsky et al. (2011) the influence of chamber volume and the height of the liquid over the orifice outlet on frequency of bubble departure have been investigated. There has been observed that increase of the chamber volume increases the time period between two subsequent bubbles. The increase in height of the liquid over the orifice outlet leads also to the increase of time period between the subsequent bubbles. In Ruzicka et al. (2009a) for investigation of bubble formation and liquid movement inside the orifice the high-speed photography and video techniques have been used. The oscillations of the gas-liquid interface inside the orifice have been analyzed. It has been shown that the gas-liquid interface inside the orifice modifies the duration of time periods between subsequent bubbles. Time period between subsequent bubbles decreases when the number of gas-liquid interface oscillations decreases.

The phenomena of liquid movement inside the orifice or nozzle have been modelled by many researches (Ruzicka et al. (2009b), Dukhin et al. (1998a), Koval'chuk et al., 1999). In Ruzicka et al. (2009b) the gas-liquid interface oscillations inside the orifice, during the waiting time, have been investigated. The process was divided into two phases. The first phase was the bubble growth and the second phase was the liquid flow inside the orifice. The liquid flow has been described by the equation of motion of mass centre of the liquid filling the orifice. Results obtained from the model have been compared with the experimental results presented in Ruzicka et al. (2009a). In Dukhin et al. (1998b) a model describing the changes of pressure distribution along the capillary and its impact on the time of liquid movement inside the nozzle has been proposed. The model takes into account the Hagen-Poiseuille equation describing the relationship between the liquid flow rate and its viscosity, pressure gradient and the nozzle geometry (length and diameter). There has been found that the maximum liquid penetration of the nozzle is dependent on the capillary pressure. The increase in gas pressure supplied to the nozzle causes the removing of liquid from the nozzle. It was also found that the time of the interface motion is longer than the time of gas pressure growth in the gas supply system. In Dukhin et al. (1998a) a model describing the gas pressure changes in the nozzle during the bubbles detachment

and gas - liquid interface position inside the nozzle has been proposed. The model is based on the simplified Navier-Stokes equations (it includes the liquid mass and momentum conservation equations). Gas was supplied to the system in periodic and aperiodic way. In the paper a relationship between the amplitude and frequency of liquid movement in the nozzle and gas pressure changes have been proposed. There has been shown that when the amplitude of pressure oscillations decreases the frequency of these oscillations increases. It was also found that the length of liquid penetration inside the nozzle decreases when the gas pressure increases. The model based on the capillary equation and equation of pressure changes in the capillary has been presented in (Koval'chuk et al., 1999). A capillary equation was based on Newton's second law for the motion of the mass centre of the liquid inside the capillary. The depth of liquid penetration inside the nozzle and duration of this process have been analyzed.

In the present study the dynamics of the liquid flow inside the glass nozzle in the process of subsequent bubble departures has been investigated experimentally. The impact of the dynamics of changes of the depth of nozzle penetration by the liquid on the process of bubbles detachment has been analyzed. During the experiment it has been simultaneously recorded: changes of the depth of the nozzle penetration by the liquid, air pressure, and shape of bubble trajectory directly over the nozzle (in the distance of 30 mm). The air volume flow rate was in the range 0.00632 - 0.0381 l/min. For such volume flow rates the bubbles do not coalesce.

2. EXPERIMENTAL SETUP AND MEASUREMENT TECHNIQUE

In the experiment bubbles were generated in tank (300x150x700 mm) - from glass nozzle with inner diameter equal to 1 mm. The experimental setup has been shown in Fig.1.

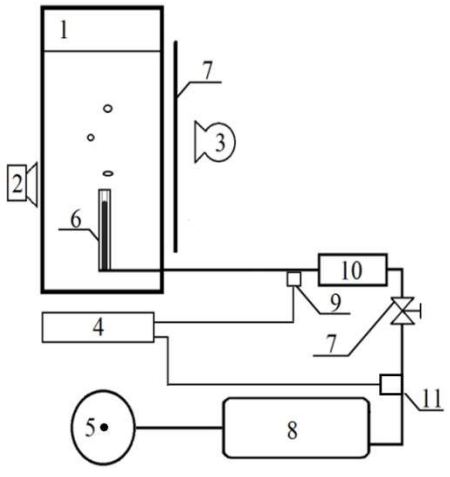

Fig. 1. Experimental setup: 1 – glass tank, 2 – camera, 3 – light source, 4 – computer acquisition system, 5 – air pump, 6 – glass nozzle, 7 - air valve, 8 – air tank, 9, 11 – pressure sensor, 10 – flow meter

The nozzle was placed at the bottom of the tank. The tank was filled with distilled water, with temperature about $20\,^{o}\mathrm{C}$. The temperature was constant during the experiment. The air pressure fluctuations have been measured using the silicon pressure sensor MPX12DP. The air volume flow rate was measured using the flow meter and was changed from 0.00632 to 0.0381 l/min. For such volume flow range the bubbles do not coalesce and the maximum depth of liquid penetration inside the nozzle was in the range between 2 mm and 20 mm. The pressure was recorded using the data acquisition system DT9800 series USB Function Modules for Data Acquisition Systems with sampling frequency of 2 kHz.

The bubble departures and liquid movement inside the nozzle were recorded with a high – speed camera – CASIO EX FX 1. The duration of each video was 20s. The recorded videos (600 fps) in gray scale have been divided into frames (Fig.2). The depth of liquid penetration inside the nozzle was measured using a computer program. The program counts on each frame the number of pixels with high brightness. The brightness threshold was different for each video. The calibration has been done by multiplication of all elements of time series by coefficient which value has been estimated using the detailed analysis of subsequent frames during the first cycle of nozzle penetration by liquid. For the selected gas flow rate, the length of the each time series was about 12 000 samples. In Fig. 2 the length of liquid penetration inside the nozzle and the bubble departures are shown. In order to better illustrate the length of liquid nozzle penetration the part of nozzle filled with a gas has been marked by continue black line. In the frames 1-6 it is visible the decrease of the length of liquid penetration inside the nozzle - the liquid is removed from the nozzle. Frames 7-12 show the bubble growth process, at frame 12 it is shown a moment of bubble departure. The frames 13 - 19 show the increase of the length of liquid penetration inside the nozzle. Above the nozzle it is visible the bubble movement. The maximum length of liquid penetration inside the nozzle in frame 19 is equal to 10 mm.

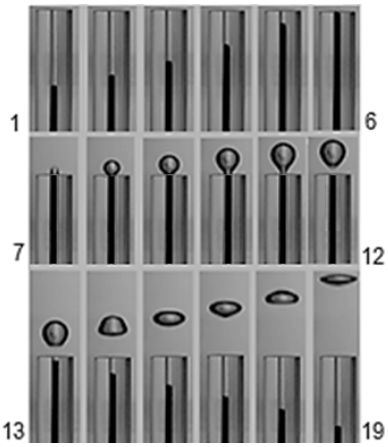

Fig. 2. The length of liquid penetration inside the nozzle and the bubble departures for air volume flow rate q = 0.0085 l/min

The example of recorded time series of changes of the length of liquid penetration inside the nozzle is shown in Fig. 3. In the time series the two time periods may be distinguished. These periods have been marked with 'I' and 'II' symbols. In the first period, the oscillations are periodic or quasi periodic. The amplitude of changes of the length of liquid penetration inside the nozzle is approximately the same for subsequent departing bubbles. In the second period (II in Fig.3), the amplitude of changes of the length of liquid penetration inside the nozzle significant varies for subsequent departing bubbles.

Time series of the length of liquid penetration inside the nozzle were obtained with using a high speed camera (600 fps) but the air pressure changes have been recorded using a data acquisition system (2 kHz). For synchronization of such recorded time series an additional system laser - phototransistor connected to data acquisition station has been used. The moment of appearance of the laser beam on the recorded film and increase of the voltage on the phototransistor was treated as the beginning of synchronized time series (the changes of pressure and the length of liquid penetration inside the nozzle).

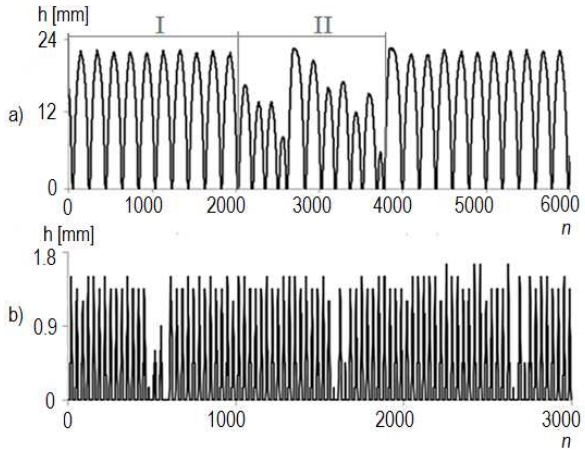

Fig. 3. Time series of changes in the position of air-liquid interface inside the glass nozzle for two gas volume flow rates, a) q = 0.0063 l/min, b) q = 0.0381 l/min

The trajectories of departing bubbles were reconstructed by computer program from recorded video. The Sobel filter has been used to identify the bubbles on the frames. Because the Sobel algorithm identifies only the boundary of the bubble, therefore the additional algorithm to fill interior of the detected bubble by black pixels has been used. This program marked the mass centre of bubble and recorded the changes of its position. The mass centre has been calculated according to the following formula:

$$x_c = \frac{\Sigma_i \, \Sigma_j \, k}{s}, \text{ where k} = \begin{cases} i \text{ for black pixels} \\ 0 \text{ for otherwise} \end{cases} \quad (1)$$

$$y_c = \frac{\Sigma_i \, \Sigma_j \, k}{s}, \text{ where k} = \begin{cases} j \text{ for black pixels} \\ 0 \text{ for otherwise} \end{cases} \quad (2)$$

where: s denotes the area of the bubble picture, x_c, y_c coordinates of the centre of mass

The example of obtained trajectories is shown in Fig. 4.

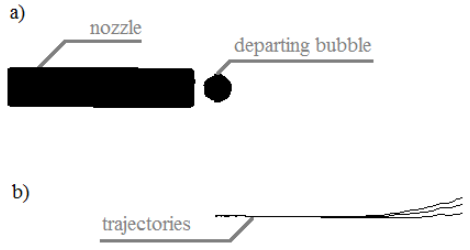

Fig. 4. Technique of bubble trajectories reconstruction: a) the black and white image of nozzle and departing bubble; b) the trajectories of three subsequent bubbles for air volume flow rate q = 0.00632 l/min

3. DATA ANALYSIS

The frequency of bubble departures has been estimated using the FFT method. The results of analysis are shown in Fig. 5. The dominant frequency of power spectrum is equal to the mean frequency of bubble departures. For q = 0.00632 l/min (Fig. 5a) the ratio between first dominate frequency and the second one is greater than in case presented in Fig. 5b. It means that when the air volume flow rate increases, the bubble departure becomes more non periodic (more chaotic).

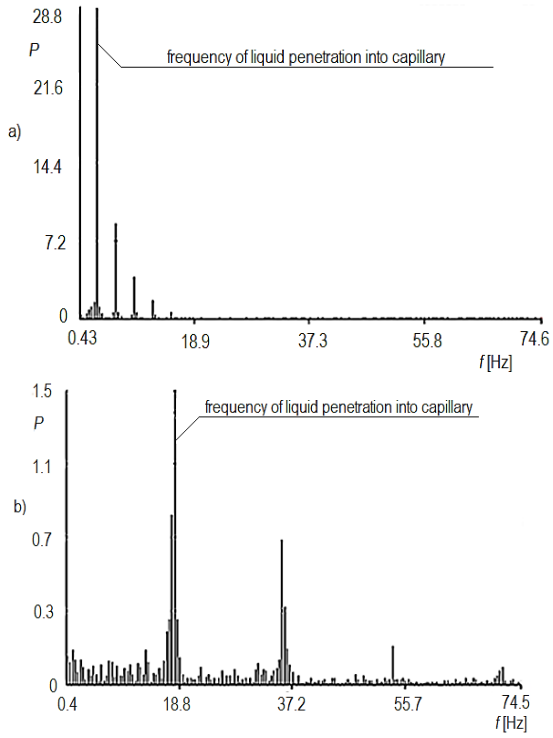

Fig. 5. Power spectrums P of time series changes in the position of air-liquid interface inside the glass nozzle: a) q = 0.00632 l/min, b) q = 0.0381 l/min (Dzienis P. et al.)

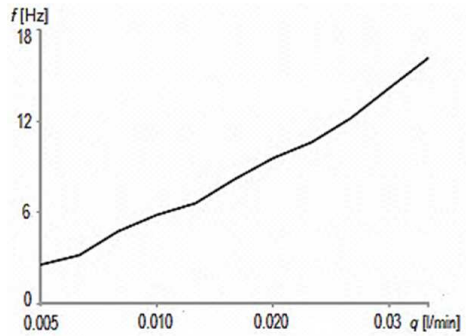

Fig. 6. The mean frequency of bubble departures f for different gas volume flow rates

Using the FTT method the mean frequency of bubble departures, f, for different air volume flow rates, q, has been determined. The results are presented in Fig.6.

In time series of the length of liquid penetration inside the nozzle the number of bubbles in two periods shown in Fig.3 and maximum value of length of liquid penetration inside the nozzle change with increase of the air volume flow rate. Typical

changes of maximum value of length of liquid penetration inside the nozzle and number of bubbles in periods I and II (Fig. 3) are shown in Fig. 7. The number of bubbles departing periodically and aperiodically, for various air volume flow rates are shown. The black bar represents the number of bubbles departing periodically in the area I (Fig. 3). The gray bar shows the number of bubbles departing aperiodically in the area marked with the symbol II in Fig. 3. The line represents the maximum length of liquid penetration inside the nozzle.

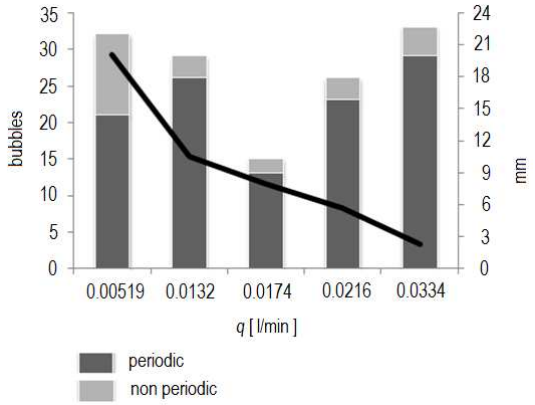

Fig. 7. Typical number of periodic and aperiodic bubbles in the time periods I and II (Fig.3) and the maximum value of length of liquid penetration inside nozzle

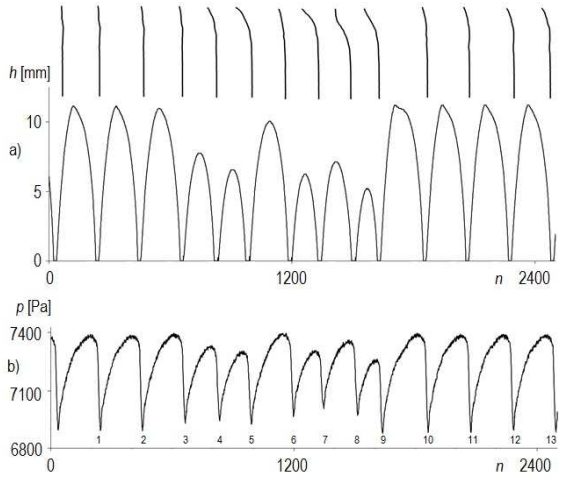

Fig. 8. Synchronized data concerning the series of bubble departures: a) the amplitude of changes in the position of air-liquid interface *h* inside the glass nozzle and the trajectories of departing bubbles for *q* = 0.0063 l/min b) the air pressure changes *p* for *q* = 0.0063 l/min

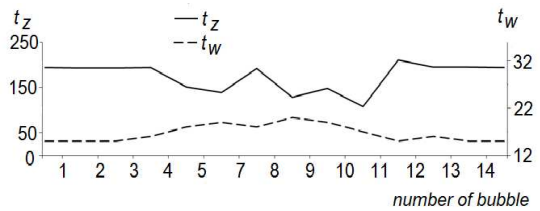

Fig. 9. The time of the growth of vapour bubbles, t_w, and the waiting time, t_z, for bubbles series presented in Fig. 8

For air flow rate, *q* = 0.00519 l/min the 21 bubbles departing periodically but 11 aperiodically. The ratio between number of aperiodically and periodically departing bubbles decreases while the air volume flow rate increases. For air volume flow rate *q* = 0.0132 l/min 26 bubbles departing periodically, and only three bubbles aperiodically. The lowest ratio between number of aperiodically and periodically departing bubbles occurs for *q* = 0.0216 l/min. For *q* = 0.0334 l/min, the ratio between number of aperiodically and periodically departing bubbles increases.

We can conclude that in the range of the air volume flow rate between 0.00519 and 0.0174 l/min, the increase of air volume flow rate is accompanied by decrease of the number of aperiodically departing bubbles. The opposite situation occurs in the range of the air volume flow rate between 0.0174 – 0.0334 l/min.

The maximum depth of liquid penetration inside the nozzle decreases while the air volume flow rate increases (Fig. 7). For *q* = 0.0334 l/min the maximum length of liquid penetration inside the nozzle was about 2 mm.

In Fig. 8 the time series representing the changes in time of the position of liquid-gas interface inside the glass nozzle (Fig. 8a), for *q* = 0.0132 l/min is shown. Above the chart the reconstruction of subsequent bubble trajectories are presented. The length of trajectories is equal to about 30 mm. In Fig. 8b the air pressure changes in gas supply system are presented. In Fig. 9 there has been shown the changes of subsequent times of: growth of bubbles and liquid movement inside the nozzle. The calculation has been made using the recorded video. The data presented in Fig. 8 and 9 refer to the same bubble series, all data are synchronized.

For the first three bubbles (Fig. 8) the time changes of the gas-liquid interface position inside the nozzles after subsequent bubble departures are similar to a periodic function. For these bubbles the maximum value of air pressure in the subsequent cycles are similar. The minimum value of air pressure reached in the subsequent cycles are similar only for the first two bubbles. Liquid flow in nozzle after third bubble begins at higher pressure, in comparison with the previous (second) bubble. Trajectories of bubbles 1-3 are similar to straight lines. For the third bubble, its growth time is longer in comparison with previous bubbles. The beginning of aperiodic bubble departures is accompanied with the rise of the time of growth bubble. For the bubbles 4, 5 (Fig. 8) the maximums of length of liquid penetration inside the nozzle and amplitudes of air pressure changes are smaller than for the previous bubbles. The liquid penetration inside the nozzle and bubble growth begins at lower air pressure. The shape of the trajectories of the bubbles 4, 5 deviates from the straight line. The time of liquid penetration inside the nozzle and bubble growth changes for subsequent cycles of growth bubbles. Bubble growth time is longer but the time of liquid penetration inside the nozzle is smaller in comparison with periodically departing bubbles (1 and 2, Fig. 8). After departure of bubble 5 the maximum value of liquid penetration depth inside the nozzle and amplitude of pressure changes increase. The liquid penetration inside the nozzle starts at higher pressure than for bubbles 4 and 5 and is close to the pressure obtained for bubbles 1-3. The trajectory of the bubble 6 is similar to the trajectory of bubbles 1-3 – it is similar to straight line. The time of liquid penetration inside the nozzle increases and is close to the times characteristic for cycles 1-3. Bubble growth time becomes smaller in comparison with bubbles 4 and 5, but it is still higher than for bubbles 1-3. The maximum value of liquid penetration inside the nozzle and amplitude of air pressure changes for bubbles 7-9 are smaller than for previous bubbles. The bubbles 7 and 8 depart at higher pressure, while the liquid penetration inside the nozzle starts at pressure lower than for bubble 6. For the bubble 9, the minimum value of air pressure

reaches the lowest value. The trajectories of bubbles 7-9 are not similar to straight lines. Times of liquid penetration inside the nozzle are lower than for bubbles 1-3 and 6. But times of growth of bubbles (7-9) are longer than for previous bubbles. The maximum value of liquid penetration inside the nozzle appearing before the bubble 10 is the lowest in analyzed time series. For the bubbles 11-13 are similar for values appearing for bubbles 1-3. The amplitudes of air pressure changes are greater than the amplitude of pressure changes for the previous bubbles, and are similar to these ones reached for bubbles 1-3. Reconstructions of bubble trajectories for these bubbles are more different from straight line in comparison with the previous bubbles. The time of liquid penetration inside the nozzle after the bubble 10 is the longest and the time of bubble growth is the smallest in bubbles time series under consideration. For bubbles 11 -13 the times of bubble growth and times of liquid penetration inside the nozzle are similar to times characteristic for bubbles 1-2. The periodic bubble departures begin when the duration of liquid penetration inside the nozzle increases and time of bubble growth decreases (bubble 11, Fig. 10).

We can conclude that the shapes of the trajectories of the departing bubbles are correlated with the maximum values of liquid penetration inside the nozzle. Straightening the trajectories of bubbles precedes the appearance of aperiodical bubble departures. Aperiodic changes of the maximum values of liquid penetration inside the nozzle appear together with significant deviations of the bubble trajectories. The periodic bubble departures lead to straightening the trajectories of bubbles.

The result presented in Fig. 10 shows that the maximum value of liquid penetration inside the nozzle is determined by highest value of air pressure changes. The time of bubble growth is determined by the minimum value of air pressure changes during the cycle of the bubble growth.

4. NONLINEAR ANALYSIS

The results presented in Fig. 7 show that increase of the air volume flow rate causes the changes of the ratio between number of bubbles in periods I and II (in Fig.3). In the period I the bubbles depart periodically, but in the period II the bubbles depart aperiodically. In order to evaluate the periodicity of bubble departures, the nonlinear analysis of time series of changes of the length of liquid penetration inside the nozzle in periods I and II has been carried out. The following elements of nonlinear analysis: attractor reconstruction, autocorrelation correlation function, correlation dimension and the largest Lyapunov exponent have been used.

The trajectories of nonlinear dynamic system in the phase space form objects called strange attractors of the structure resembling a fractal (Otto, 19978; Wolf et al., 1985). The analysis of strange attractor gives information about the properties of dynamic system such as system complexity and its stability. In nonlinear analysis the reconstruction of attractor in a certain embedding dimension has been carried out using the stroboscope coordination. In this method subsequent co-ordinates of attractor points have been calculated basing on the subsequent samples, between which the distance is equal to time delay τ. The nonlinear analysis of the experimental data is initiated by determining the time delay τ. For that purpose, the autocorrelation function, C, is usually calculated. The value of the time delay τ is determined from the condition $C(\tau)\sim 0.5*C(0)$ (Schuster H.G., Otto E.).

In Fig. 10 are shown the examples of 3D attractors reconstructions. The values of τ have been calculated using the autocorrelation function.

The correlation dimension D_2 is one of the characteristics of attractors, which allows to identify the structure of attractors. It is defined by the following expression (Schuster, 1993; Otto, 1997):

$$D_2 = \lim_{d\to 0} \frac{1}{\ln(d)} lnC^2(d) \tag{3}$$

where: $C^2(d) = \frac{1}{N}\sum_i \left[\frac{1}{N}\sum_j \theta\left(d - |x_i - x_j|\right)\right]$, d – distance in embedding space, N – number of points, θ – Heaviside's step function that determines the number of attractor point pairs of the distance shorter than d.

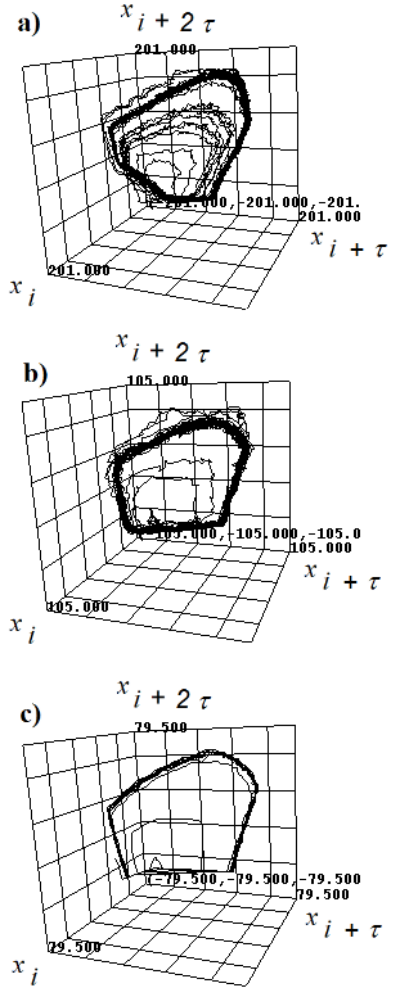

Fig. 10. 3D attractors for liquid penetration inside the nozzle time series: a) q = 0.00519 l/min and τ = 30, b) q = 0.0132 l/min and τ = 16, c) q = 0.0174 l/min and τ = 12

The correlation dimension allows to estimate the number of independent variables describing the phenomenon under consideration. This number is estimated as the lowest integer number greater than the correlation dimension. In Fig.11 the results of calculation of correlation dimension are presented. Obtained results show that correlation dimension of all time series is less than three. It means that three independent variables are enough to describe the behaviour of liquid movement inside the nozzle.

The another important characteristics of attractors is the largest Lyapunov exponent. In this case two points on the attractor immersed in M dimensional space have been selected. The distance between these points $d(x_j)$ is at least the one orbiting period.

After the passage of certain time the distance between the selected points has been calculated again and denoted as $d(x_{j+1})$. The largest Lyapunov exponent has been calculated according to the following formula:

$$L = \frac{1}{t}\sum_{j=1}^{m} \log \frac{d(x_{j+1})}{d(x_j)} \quad (4)$$

where: m – number of examined points, t – time of evolution.

The largest Lyapunov exponent allows calculation of time period $(1/L)$ of long time memory in the system in which the process of stability loss occurs. The comparison between the value of long time memory calculated from the largest Lyapunov exponent and the average time of the single bubble growth ($1/f$) is presented in Fig.10 ($(1/L)/(1/f) = f/L$).

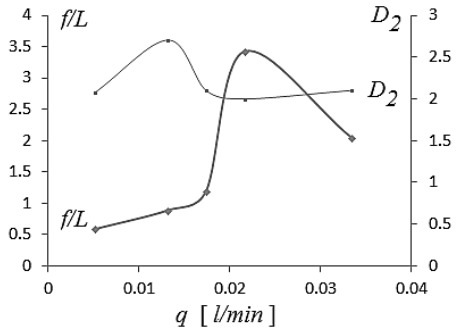

Fig. 11. The correlation dimension and largest Lyapunov exponent of changes in the position of air-liquid interface in glass nozzle versus air volume flow rate

The ratio f/L (f – the frequency of bubble departures, L – largest Lyapunov exponent) specifies the number of bubbles in which the stability of system is lose. For air volume flow rate q = 0.00519 l/min and q = 0.0132 l/min the ratio f/L has a value below 1. Because in case under consideration the time of bubble growth is about 10 times smaller in comparison with the duration of liquid penetration inside the nozzle, therefore results can be concluded that the aperiodical bubble departures are caused by the sensitivity to initial and boundary conditions of the liquid movement inside the nozzle.

5. CONCLUSIONS

The main aim of investigation was to analyze the influence of dynamics of liquid movement inside the nozzle on the dynamics of bubble departure. It has been analyzed: the liquid penetration inside the nozzle, air pressure changes in gas supply system and bubble trajectories shape. The results of analysis can be summarized as follows:

- increase of air volume flow rate is accompanied by increase of frequency of bubble departures and decrease of maximum values of liquid penetration (during the single bubble cycle) inside the nozzle;
- for all air volume flow rates (in the experiment) the time periods with periodic and aperiodic bubble departures appeared. The duration of these intervals varies with air volume flow rate;
- changes of maximum values of liquid position inside the nozzle are associated with changes of the bubble trajectories. Straightening the trajectory precedes the appearance of periodical and aperiodical time periods of bubble departures. The aperiodic bubble departures are accompanied by a significant deviation of bubbles trajectory from a straight line;
- changes of the amplitudes of air pressure (during the single bubble cycles) are correlated with the duration of liquid penetration inside the nozzle and times of the bubble growth. The maximum values of liquid penetration inside the nozzle are determined by highest value of air pressure changes. The times of bubble growths are correlated with the minimum values of air pressure changes;
- the aperiodic bubble departures begin when the time of bubble growth increased;
- the periodic bubble departures begin when the duration of liquid penetration inside the nozzle increase and time of bubble growth decreased;
- the aperiodical bubble departures are caused by the sensitivity to initial and boundary conditions of the liquid movement inside the nozzle;
- the correlation dimension analysis showed that three independent variables are enough to describe the behaviour of liquid movement inside the nozzle. These independent variables can be: liquid velocity, liquid position in nozzle and gas pressure in the nozzle.

REFERENCES

1. **Cieslinski J.T., Mosdorf R.** (2005), Gas bubble dynamics experiment and fractal analysis, *Int. J. Heat Mass Transfer*, Vol. 48, No. 9, 1808–1818.
2. **Dukhin S.S., Koval'chuk V.I., Fainerman V.B., Miller R**. (1998a), Hydrodynamic processes in dynamic bubble pressure experiments Part 3. Oscillatory and aperiodic modes of pressure variation in the capillary, Colloids and Surfaces A, *Physicochemical and Engineering Aspects*, Vol. 141, 253–267.
3. **Dukhin S.S., Mishchuk N.A., Fainerman V.B., Miller R.** (1998b), Hydrodynamic processes in dynamic bubble pressure experiments 2. Slow meniscus oscillations, Colloids and Surfaces A: *Physicochemical and Engineering Aspects*, Vol. 138, 51–63.
4. **Dzienis P., Wyszkowski T., Mosdorf R.** (2012), Nonlinear analysis of liquid movement inside the glass nozzle during air bubble departures in water, *Advances in Chemical and Mechanical engineering*, 133-137.
5. **Koval'chuk V.I., Dukhin S.S., Fainerman V.B., Miller R.** (1999), Hydrodynamic processes in dynamic bubble pressure experiments, 4. Calculation of magnitude and time of liquid penetration into capillaries, Colloids and Surfaces A: *Physicochemical and Engineering Aspects*, Vol. 151, 525–536.
6. **Mosdorf R., Shoji M.** (2003), Chaos in bubbling - nonlinear analysis and modelling, Chem. Eng. Sci., Vol. 58, 3837–3846.
7. **Otto E.,** (1997), *Chaos in Dynamical Systems*. WNT (in Polish).
8. **Ruzicka M.C., R. Bunganic R., Drahos J.** (2009b) , Meniscus dynamics in bubble formation. Part II: *Model, Chemical Engineering Research and Design*, Vol. 87, 1357–1365.
9. **Ruzicka, M.C., Bunganic, R. Drahos, J.** (2009a), *Meniscus dynamics in bubble formation*, Part I: *Experiment. Chem. Eng. Res. Des.,* Vol. 87, 1349–1356.
10. **Schuster H.G.** (1993), *Deterministic Chaos. An Introduction*, PWN, Warszawa 1993 (in Polish).
11. **Stanovsky P., Ruzicka M.C., Martins A., Teixeira J.A** (2011), Meniscus dynamics in bubble formation: A parametric study, *Chemical Engineering Science*, Vol. 66, 3258–3267.
12. **Wolf A., Swift J.B., Swinney H.L., Vastano J.A.** (1985) Determining Lyapunov Exponent from a Time series, *Physica-D*, Vol. 16, 285-317.
13. **Zang L., Shoji M.,** (2001), Aperiodic bubble formation from a submerged orifice, *Chemical Engineering Science*, Vol. 56, 5371-5381.